Advances in Nano Research, *Vol. 17, No.1 (2024) 19-32*
https://doi.org/10.12989/anr.2024.17.1.019

An innovative approach for analyzing free vibration in functionally graded carbon nanotube sandwich plates

Shahabeddin Hatami*, Mohammad J. Zarei[a] and Seyyed H. Asghari Pari[a]

Department of Civil Engineering, Yasouj University, Iran

(*Received October 14, 2023, Revised June 14, 2024, Accepted June 18, 2024*)

Abstract. Functionally graded-carbon nanotube (FG-CNT) is expected to be a new generation of materials with a wide range of potential applications in technological fields such as aerospace, defense, energy, and structural industries. In this paper, an exact finite strip method for functionally graded-carbon nanotube sandwich plates is developed using first-order shear deformation theory to get the exact natural frequencies of the plates. The face sheets of the plates are made of FG-CNT with continuous and smooth grading based on the power law index. The equations of motion have been generated based on the Hamilton principle. By extracting the exact stiffness matrix for any strip of the sandwich plate as a non-algebraic function of natural frequencies, it is possible to calculate the exact free vibration frequencies. The accuracy and efficiency of the current method is established by comparing its findings to the results of the literature works. Examples are presented to prove the efficiency of the generated method to deal with various problems, such as the influence of the length-to-height ratio, the power law index, and a core-to-face sheet thickness of the single and multi-span sandwich plates with various boundary conditions on the natural frequencies. The exact results obtained from this analysis can check the validity and accuracy of other numerical methods.

Keywords: exact finite strip method; first order shear deformation theory; free vibration; functionally graded-carbon nanotube; sandwich plate

1. Introduction

Sandwich structures are a class of laminated composites and consist of two main parts: the core and the face sheets. The face sheets are resistant to transverse and in-plane loads, and the core withstands shear forces. Functionally graded-carbon nanotube (FG-CNT) are progressed non homogeneous composites with various phases of component. The material characteristics of FG-CNTs can be unidirectional or bidirectional in either the length or thickness. Therefore, their physical properties, like the modulus of elasticity are variable. The FG-CNTs have comprehensive applications in aerospace, civil engineering, biotechnology, mechanical engineering, and automotive structures (Rout and Hota 2023, Gholami *et al.* 2023, Zhao *et al.* 2022, Garg *et al.* 2022, Barati *et al.* 2022, Gao *et al.* 2022, Yang *et al.* 2020, Yang and He 2019, Riahi *et al.* 2019, Soltani *et al.* 2016).

The exact Finite Strip Method (FSM) of free vibration analysis of the sandwich plates has recently been extended. In the exact FSM, the two-dimensional plate is divided into a few strips. Interpolation of displacement in both in-plane directions is done utilizing a set of shape functions generated in longitudinal and transverse directions. The shape functions for the transverse direction are assumed to be trigonometric terms. On the other hand, in the longitudinal direction, exponential functions are taken. The finite strip method, pioneered by Cheung (1968) is an efficient tool for analysing structures with a common geometric platform and simple boundary conditions. Initially, the finite strip method was designed for rectangular plate problems similar to Levy's solution; Timoshenko and Woinowsky-Krieger (1959). Wittrick and Williams (1974) proposed the exact strip method for plate structures based on Levy-type solutions. The finite strip approach can apply to the vibration and stability challenges of shells and plates. Hatami *et al.* (2008) used the classical theory of plates to calculate the free vibration of moving viscoelastic plates. Bahrami and Hatami (2016) investigated the free vibration of moderately thick Levy-type plates, based on the theory of first-order shear deformation. They presented comprehensive results for out-of-plane natural frequencies and transverse displacements of moderately thick rectangular plates with different combinations of boundary conditions to be used as benchmarks for comparing the accuracy and precision of numerical methods.

Many researchers have been interested in the free vibration of functionally graded (FG) material structures, including functionally graded-carbon nanotube (FG-CNT) sandwich plates. Wu *et al.* (2015) investigated the free vibration of sandwich structures with a strong core and face sheets made of functionally graded carbon nanotube reinforced composite (FG-CNTRC). Dash *et al.* (2018) examined modal frequency responses for FG sandwich panels. Meksi *et al.* (2019) explored the vibration reactions of the FG sandwich plate by developing a theory of shear deformation plate. Kumar *et al.* (2021) examined vibration analysis for plates of functional gradation (FG) of linearly

*Corresponding author, Associate Professor
E-mail: hatami@yu.ac.ir
[a] Master's degree in structural engineering

ISSN: 2287-237X (Print), 2287-2388 (Online)

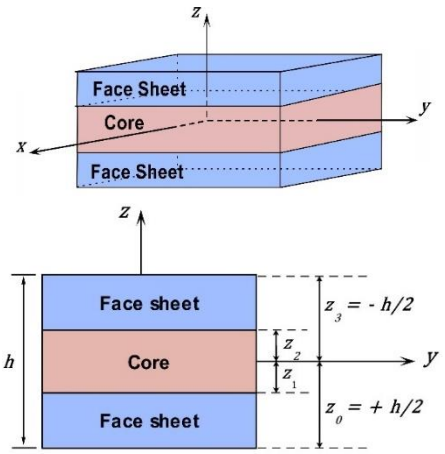

Fig. 1 Schematic representation of a sandwich plate

variable thicknesses. Hadji and Avcar (2021) examined the vibration behaviors of a FG sandwich plate. They got analytical solutions for free vibration assessment of square FG sandwich plates with difference boundary conditions. Mousavi *et al.* (2021) studied the free vibration behavior of a Porous Micro (PM) beam with Functionally Graded Piezoelectric (FGP) layers, using two trigonometric shear deformation theories - SSDBT and Tan-SDBT. Soni *et al.* (2022) devoted significant effort to examining functionally graded carbon nanotubes reinforced composite (FG-CNTRC) structures in great detail due to their advantageous vibration characteristics, and thermo-mechanical compared to traditional composites. Wu and Fang (2022) used Von-Karman theory to examine the nonlinear impact of the vibrational behavior of a non-homogeneous composition of functionally graded nanotubes via strain gradient theory and high-order Reddy beam theory. Chiker *et al.* (2023) conducted a thorough parameter-based analysis of the free vibration response of multi-layer carbon-based nano-composite-made laminated composite plates, taking into consideration both linear and nonlinear distribution of the nano-reinforcements. Carbon nanotubes, embedded in a polymer mixture and reinforced with nanotechnology, form the components of these layers. It is presumed that the CNTs are uniformly distributed (UD) or varying in proportion to their purpose means functionally graded (FG) across the ply thickness. Marandi and Karimipour (2023) applied an extended high-order approach to study the free vibration analysis of Nanoscale CNTRCs sandwich beams. The face sheets in this study are constructed of PMMA reinforced with single-wall carbon nanotubes, and a honeycomb structure is chosen as the flexible core. The skins are examined with first-order shear deformation theory. Talebi *et al.* (2023) examines the thermal free vibration of a sandwich piezoelectric agglomerated Timoshenko beam reinforced by carbon nanotubes, and the pyroelectric effect is considered. Eghbali and Hosseini (2023) investigates the axial and transverse dynamic response of carbon nanotube-reinforced composite (CNTRC) beams under moving harmonic load using higher-order shear deformation theories.

This article examines the free vibration of FG-CNT sandwich plates through the usage of the first-order shear deformation theory and the exact finite strip method. For this purpose, the plate is divided into limited strips. The stiffness matrix of each finite strip is determined in terms of free vibration frequencies and the mechanical and geometrical properties of the problem. By forming the stiffness matrix of the entire sandwich plate, possible to compute these structures' exact free vibration frequencies. This process calculates the natural frequencies of sandwich plates that have face sheets composed of graded materials that feature a continuous and smooth distribution under the power law index. By comparing the goat frequencies with the research results of other researchers, the correctness and accuracy of the developed finite strip method are confirmed. The exact outcomes from this evaluation can check the accuracy and correctness of other numerical techniques.

2. Theory and formulation of FG-CNT sandwich plates

The This research analyzes the sandwich plate, which comprises three layers, two FG-CNT face sheets, and a homogenous core. The FG-CNT sandwich plates are made of nonhomogeneous materials in thickness. Continuous functions are used to model the changes in material properties in thickness, including the modulus of elasticity and density. For each layer, the effective material properties (T) are expressed:

$$\begin{aligned} T_{fb}(z) &= T_f + \left(T_c - T_f\right) V_{fb}(z) \\ T_c(z) &= T_f + \left(T_c - T_f\right) V_c(z) \\ T_{ft}(z) &= T_f + \left(T_c - T_f\right) V_{ft}(z) \end{aligned} \tag{1}$$

where the subscript c is for core, f is for face sheet, t is for top and b is for bottom. T_{ft} and T_{fb} are the values of effective material properties in the upper and lower faces of the sandwich plate, respectively, and V is the volume fraction function. The physical reality of the structure and the clarity are two essential features for choosing the proposed volume fraction function. The volume fraction of the core and face sheets changes under the following power-law expression through the thickness of the sandwich plate:

$$\begin{aligned} V_{fb}(z) &= \left(\frac{z - z_0}{z_1 - z_0}\right)^p \quad z_0 \le z \le z_1 \\ V_c(z) &= 1 \quad z_1 \le z \le z_2 \\ V_{ft}(z) &= \left(\frac{z - z_3}{z_2 - z_3}\right)^p \quad z_2 \le z \le z_3 \end{aligned} \tag{2}$$

where $z_0, z_1, z_2 \; and \; z_3$ are the coordinates of the bottom face of the layers in z direction, as shown in Fig. 1, and the coefficient p denotes the volume fraction index (power-law) and the distribution of the material over the thickness. It is to be noted that when $p = 0$, the material properties of the sandwich plate become homogenous, and the properties can be altered linearly by choosing $p = 1$. Fig. 2 outlines the distribution models of material for two varieties of FG-CNT sandwich plates about adjustments in the volume fraction index (p). According to these models, As p increases, the material distribution on the lower side of the layer increases.

FG-CNT Sandwich plates can have different designs

according to the face sheets and core thickness. For example, the number (2-1-2) indicates a three-layer sandwich plate whose the thickness of the face sheet is double that of the core. A further example of the (2-1-1) FG-CNT sandwich plate indicates a three-layer plate with a top face thickness equivalent to the core thickness and the bottom face thickness is double the core thickness. Therefore, according to Fig. 1, in this case, we have $z_0 = h/2,\ z_1 = 0,\ z_2 = -h/4$, and $z_3 = -h/2$.

2.1 Strains and displacement

This research uses the first-order shear deformation theory (FSDT) to get the equations of motion. According to this theory, the transverse normals no longer stay perpendicular to the mid-surface when deformed (Fig. 3). Transverse shear strains that are constant across the plate thickness must be included in the theory. However, the transverse shear stresses in composite plates show a varying measure of at least quadratically across the layer thickness. As a result, a shear correction factor is needed to modifying the plate transverse shear stiffnesses (Reddy 2003).

The form of the deformation field of FSDT is:

$$\begin{aligned} u(x,y,z,t) &= u_0(x,y,t) + z\varphi_x(x,y,t) \\ v(x,y,z,t) &= v_0(x,y,t) + z\varphi_y(x,y,t) \\ w(x,y,z,t) &= w_0(x,y,t) \end{aligned} \tag{3}$$

where $u, v\ and\ w$ show the displacement of a point (x, y, z) in the x, y, and z directions. $(u_0, v_0, w_0, \varphi_x, \varphi_y)$ are unknown functions that still need to be resolved. (u_0, v_0, w_0) denote the displacement of a point in the $z = 0$ (see Fig. 3). These two functions, φ_x and φ_y are rotations of the normal to the mid-plane of the laminate with respect to the x- and y-axes respectively, as shown:

$$\begin{aligned} \varphi_x(x,y,t) &= \frac{\partial u}{\partial z} = \gamma_{xz} - \frac{\partial w_0}{\partial x} \\ \varphi_y(x,y,t) &= \frac{\partial v}{\partial z} = \gamma_{yz} - \frac{\partial w_0}{\partial y} \end{aligned} \tag{4}$$

It is important to understand that the transverse strain components γ_{xz}, and γ_{yz} are not always equal to zero in the first-order shear deformation plate theory. The strain in the middle plane of the plate can be obtained by linear functions of displacements or by non-linear functions of Euler-Lagrange equations. By ignoring non-linear terms due to their smallness, the strains related to displacement as:

$$\begin{Bmatrix} \varepsilon_x \\ \varepsilon_y \\ \gamma_{yz} \\ \gamma_{xz} \\ \gamma_{xy} \end{Bmatrix} = \begin{Bmatrix} \varepsilon_x^0 \\ \varepsilon_y^0 \\ \gamma_{yz} \\ \gamma_{xz} \\ \gamma_{xy}^0 \end{Bmatrix} + z \begin{Bmatrix} \varepsilon_x^1 \\ \varepsilon_y^1 \\ 0 \\ 0 \\ \gamma_{xy}^1 \end{Bmatrix} = \{\varepsilon^0\} + z\{\varepsilon^1\} =$$
$$\begin{Bmatrix} \frac{\partial u_0}{\partial x} + \frac{1}{2}\left(\frac{\partial w_0}{\partial x}\right)^2 \\ \frac{\partial v_0}{\partial x} + \frac{1}{2}\left(\frac{\partial w_0}{\partial y}\right)^2 \\ \frac{\partial w_0}{\partial y} + \varphi_y \\ \frac{\partial w_0}{\partial x} + \varphi_x \\ \frac{\partial u_0}{\partial y} + \frac{\partial v_0}{\partial x} + \frac{\partial w_0}{\partial x}\frac{\partial w_0}{\partial y} \end{Bmatrix} + z \begin{Bmatrix} \frac{\partial \varphi_x}{\partial x} \\ \frac{\partial \varphi_y}{\partial y} \\ 0 \\ 0 \\ \frac{\partial \varphi_x}{\partial y} + \frac{\partial \varphi_y}{\partial x} \end{Bmatrix} \tag{5}$$

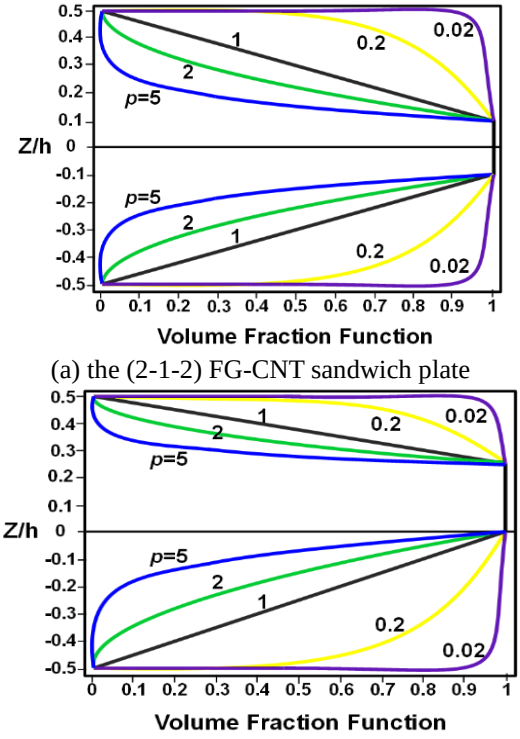

(a) the (2-1-2) FG-CNT sandwich plate

(b) the (2-1-1) FG-CNT sandwich plate

Fig. 2 Variation of volume fraction function through plate thickness for various values of the power-law index p

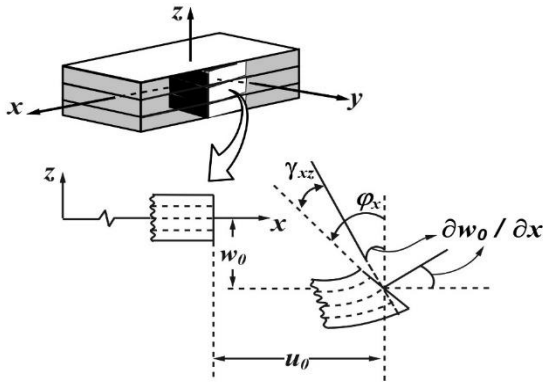

Fig. 3 Deformation of the mid-surface of sandwich plate

The membrane and bending strains of the middle surface of the plate are represented by ε^0 and ε^1, respectively. bending strains (ε^1) consist of changes in curvatures ($\varepsilon_x^1, \varepsilon_y^1$) and twist ($\gamma_{xy}^1$). In the FSDT, the membrane strains ($\varepsilon_x, \varepsilon_y, \gamma_{xy}$) are linear through the plate's thickness, while the transverse strains $(\gamma_{xz}, \text{and } \gamma_{yz})$ remain consistent. In this theory, the normal length remains constant ($\varepsilon_z = 0$).

2.2 The resultant forces and moments

The constitutive equations in plate coordinates are determined by transforming the stiffness matrix $[Q]$. The elastic stiffness matrix $[Q]$ expresses the relationship between the stresses (σ) and strains (ε). Now, by applying Hooke's law arrive:

$$\{\sigma\} = [Q]\{\varepsilon\} = [Q]\{\varepsilon^0\} + [Q]z\{\varepsilon^1\} \quad (6)$$

The force (N) and moment (M) effects are described in the sandwich plate as follows:

$$\begin{Bmatrix} N \\ M \end{Bmatrix} = \sum_{k=0}^{2} \int_{Z_k}^{Z_{k+1}} \{\sigma\} \begin{Bmatrix} 1 \\ z \end{Bmatrix} dz = \sum_{k=0}^{2} \int_{Z_k}^{Z_{k+1}} [Q]\{\varepsilon^0\} \begin{Bmatrix} 1 \\ z \end{Bmatrix} dz + \sum_{k=0}^{2} \int_{Z_k}^{Z_{k+1}} z\,[Q]\{\varepsilon^1\} \begin{Bmatrix} z \\ z^2 \end{Bmatrix} dz \quad (7)$$

where h is the plate's thickness. The moments are calculated according to the curvature and strain of the middle surface of the plate. It is also possible to rewrite the force and moment equations in matrix form as:

$$\begin{Bmatrix} N \\ M \end{Bmatrix} = \begin{bmatrix} A & B \\ B & D \end{bmatrix} \begin{Bmatrix} \varepsilon^0 \\ \varepsilon^1 \end{Bmatrix} \quad (8)$$

where $A_{ij} = \sum_{k=0}^{2} Q_{ij}^{k}\{Z_{k+1} - Z_k\}$, also called extensional stiffness terms; $B_{ij} = \frac{1}{2}\sum_{k=0}^{2} Q_{ij}^{k}\{Z_{k+1}^2 - Z_k^2\}$, also called coupling stiffness terms; $D_{ij} = \frac{1}{3}\sum_{k=0}^{2} Q_{ij}^{k}\{Z_{k+1}^3 - Z_k^3\}$, also known as bending stiffness terms; and Q_{ij} are coefficients of elastic stiffness. The sandwich plate examined in this work is symmetrical and balanced, therefore $B_{ij} = 0$; $A_{16} = 0$; $A_{26} = 0$. Also, assume that D_{16} and D_{26} are negligible, except for generally orthotropic and anisotropic multiple layers.

Despite the continuous strain between the layers, the stresses are not continuous because of the material distinction of layers, so the results of the forces (N_x, N_y, N_{xy}) and moments (M_x, M_y, M_{xy}) for a symmetrical sandwich plate are as follows:

$$\begin{Bmatrix} N_x \\ N_y \\ N_{xy} \end{Bmatrix} = \begin{bmatrix} A_{11} & A_{12} & 0 \\ A_{12} & A_{22} & 0 \\ 0 & 0 & A_{66} \end{bmatrix} \begin{Bmatrix} \frac{\partial u_0}{\partial x} + \frac{1}{2}(\frac{\partial w_0}{\partial x})^2 \\ \frac{\partial v_0}{\partial x} + \frac{1}{2}(\frac{\partial w_0}{\partial y})^2 \\ \frac{\partial u_0}{\partial y} + \frac{\partial v_0}{\partial x} + \frac{\partial w_0}{\partial x}\frac{\partial w_0}{\partial y} \end{Bmatrix}$$

$$\begin{Bmatrix} M_x \\ M_y \\ M_{xy} \end{Bmatrix} = \begin{bmatrix} D_{11} & D_{12} & 0 \\ D_{12} & D_{22} & 0 \\ 0 & 0 & D_{66} \end{bmatrix} \begin{Bmatrix} \frac{\partial \varphi_x}{\partial x} \\ \frac{\partial \varphi_y}{\partial y} \\ \frac{\partial \varphi_x}{\partial y} + \frac{\partial \varphi_y}{\partial x} \end{Bmatrix} \quad (9)$$

In addition, the transverse shear forces (Q_x, Q_y) produced by σ_{xz} and σ_{yz}, respectively, are obtained as follows

$$\begin{Bmatrix} Q_y \\ Q_x \end{Bmatrix} = k_s \sum_{k=0}^{2} \int_{Z_k}^{Z_{k+1}} \begin{Bmatrix} \sigma_{yz} \\ \sigma_{xz} \end{Bmatrix} dz = k_s \begin{bmatrix} A_{44} & 0 \\ 0 & A_{55} \end{bmatrix} \begin{Bmatrix} \frac{\partial w_0}{\partial y} + \varphi_y \\ \frac{\partial w_0}{\partial x} + \varphi_x \end{Bmatrix} \quad (10)$$

The transverse shear in the FSDT is constant. Evidently, the permanent transverse shear is an overall approximation of the real stress field, which is at least of the quadratic across the thickness. The shear correction factor, k_s, for a general laminate is pertains to the properties of the lamina and the scheme of lamination. The elastic stiffness matrix $[Q_{ij}^{k}]$ is as follows:

$$Q_{ij}^{k} = \begin{bmatrix} \frac{E_1^k(z)}{1-\upsilon_{12}^k\upsilon_{21}^k} & \frac{\upsilon_{12}^k E_2^k(z)}{1-\upsilon_{12}^k\upsilon_{21}^k} & 0 & 0 & 0 & 0 \\ \frac{\upsilon_{12}^k E_2^k(z)}{1-\upsilon_{12}^k\upsilon_{21}^k} & \frac{E_2^k(z)}{1-\upsilon_{12}^k\upsilon_{21}^k} & 0 & 0 & 0 & 0 \\ 0 & 0 & 0 & 0 & 0 & 0 \\ 0 & 0 & 0 & G_{23}^k(z) & 0 & 0 \\ 0 & 0 & 0 & 0 & G_{13}^k(z) & 0 \\ 0 & 0 & 0 & 0 & 0 & G_{12}^k(z) \end{bmatrix} \quad (11)$$

where $E^k(z)$ is an elastic modulus, $G^k(z)$ is the k-layer shear modulus of the sandwich plate, and υ is the Poisson ratio. Using the first order shear deformation theory (FSDT), the equations of motion can be computed through Hamilton's principle of dynamic virtual displacements as shown:

$$\begin{aligned} \delta w_0 &: \frac{\partial Q_x}{\partial x} + \frac{\partial Q_y}{\partial y} - k_0 w_0 + \tilde{N}(w_0) + q = I_0 \ddot{w}_0 \\ \delta \varphi_y &: \frac{\partial M_{xy}}{\partial x} + \frac{\partial M_y}{\partial y} - Q_y = I_2 \ddot{\varphi}_y + I_1 \ddot{v}_0 \\ \delta \varphi_x &: \frac{\partial M_x}{\partial x} + \frac{\partial M_{xy}}{\partial y} - Q_x = I_2 \ddot{\varphi}_x + I_1 \ddot{u}_0 \end{aligned} \quad (12)$$

where q is external distributed force, t is the time, k_0 is Winkler modulus, and $\ddot{\Delta} = \frac{\partial^2 \Delta}{\partial t^2}$. The the special character $\tilde{N}(w_0) = \frac{\partial}{\partial x}\left(N_x \frac{\partial w_0}{\partial x} + N_{xy}\frac{\partial w_0}{\partial y}\right) + \frac{\partial}{\partial y}\left(N_{xy}\frac{\partial w_0}{\partial x} + N_y \frac{\partial w_0}{\partial y}\right)$. The current formulation uses the symbol (δ) as a variational operator, and (I_0, I_1, I_2) are the mass moments of inertia as:

$$\begin{Bmatrix} I_0 \\ I_1 \\ I_2 \end{Bmatrix} = \sum_{k=0}^{2} \rho_k \begin{Bmatrix} (z_{k+1} - z_k) \\ \frac{1}{2}(z_{k+1}^2 - z_k^2) \\ \frac{1}{3}(z_{k+1}^3 - z_k^3) \end{Bmatrix} \quad (13)$$

where ρ_k is the mass density of the k-layer carbon nanotube sandwich plate.

2.3 Free vibration equation of the FG-CNT sandwich plate

At first, the equations governing a symmetric multi-layered plate are extracted. Since sandwich plates are a particular type of multilayer plates, applying the conditions related to sandwich plates, the equations of these plates are calculated based on the first-order shear theory. Sandwich plates can be considered a particular type of multilayer plate, as shown in Fig. 1. Here, the following assumptions and restrictions (Reddy 2003) are used:

- The layers are perfectly connected.
- The thickness of each layer is uniform.
- Every layer is made from a linearly elastic material.
- The displacements and strains are small.
- The effect of rotatory inertia is negligible.
- The straight lines perpendicular to the mid-surface will stay straight, and no occurrence of elongation, even after being deformed. This supposes that the transverse displacement is unrelated to the transverse coordinate and that the normal transverse strain is zero.
- After deformation, the transverse normals to no longer

be perpendicular to the mid-surface. This assumption leads to transverse shear strains being not zero.

Interpolation of displacement in the two in-plane directions is established by a set of determined shape functions in the longitudinal and transverse directions. Both opposite sides of the sandwich plate have been arranged in an S-S boundary condition at $x = 0$ and $x = L$. The shape functions that comply with these regulations can be composed as:

$$\begin{aligned} w_0(x,y,t) &= \sum_{m=1}^{\infty} w_m(y)\, Sin(\alpha x) e^{i\omega t} \\ \varphi_y(x,y,t) &= \sum_{m=1}^{\infty} \varphi_{y_m}(y)\, Sin(\alpha x) e^{i\omega t} \\ \varphi_x(x,y,t) &= \sum_{m=1}^{\infty} \varphi_{x_m}(y)\, Cos(\alpha x) e^{i\omega t} \end{aligned} \tag{14}$$

where $\alpha = (m\,\pi)/L,\ m = 1,2,3,\ldots,\infty$, and ω is the unknown natural frequency. Inserting Eqs. (9) and (10), into Eq. (12) produces a collection of three differential equations:

$$\begin{aligned} &\delta w_0\colon\ k_s A_{55}\left(w_m''(y) + \varphi_{x_m}'(y)\right) \\ &+k_s A_{44}\left(-\alpha^2 w_m(y) - \alpha\varphi_{y_m}(y)\right) = -I_0\omega^2 w_x(y) \\ &\delta\varphi_y\colon D_{66}\left(\alpha\,\varphi_{x_m}'(y) + \varphi_{y_m}''(y)\right) + D_{12}\left(\alpha\varphi_{x_m}'(y)\right) \\ &+D_{22}\left(-\alpha^2\varphi_{y_m}\right) - k_s A_{55}\left(\alpha\, w_m(y) + \varphi_{y_m}(y)\right) \\ &= -I_2\omega^2\varphi_{y_m}(y) \\ &\delta\varphi_x\colon D_{11}\left(\varphi_{x_m}''(y)\right) - D_{12}\left(\alpha\,\varphi_{y_m}'(y)\right) \\ &+D_{66}\left(-\alpha^2\,\varphi_{x_m} - \alpha\,\varphi_{y_m}'(y)\right) \\ &-k_s A_{55}\left(w_m'(y) + \varphi_{x_m}(y)\right) = -I_2\omega^2\varphi_{x_m}(y) \end{aligned} \tag{15}$$

where $k_0 = \tilde{N}(w_0) = q = 0$. To solve simultaneous coupled equation (Eq. (15)), they are first sorted according to the order of that equation by changing the following variables:

$$\begin{aligned} &\bar{A} = \left(\frac{k_s A_{44}\alpha^2 - I_0\omega^2}{(k_s A_{55})}\right), \bar{B} = \left(\frac{k_s A_{44}\alpha}{(k_s A_{55})}\right),\ \bar{C} = \left(\frac{-k_s A_{55}}{(k_s A_{55})}\right), \\ &\bar{E} = \left(\frac{k_s A_{44}\alpha}{D_{66}}\right),\ \bar{M} = \left(\frac{k_s A_{55}}{D_{11}}\right),\ \bar{F} = \left(\frac{D_{22}\alpha^2 + k_s A_{44} - I_2\omega^2}{D_{66}}\right), \\ &\bar{H} = \left(\frac{(-D_{66}\alpha - D_{12}\alpha)}{D_{66}}\right), \qquad \bar{N} = \frac{(D_{12}\alpha + D_{66}\alpha)}{D_{11}}, \\ &\bar{P} = \left(\frac{D_{12}\alpha^2 + k_s A_{55} - I_2\omega^2}{D_{11}}\right). \\ &w_m''(y) = \bar{A}\, w_m(y) + \bar{B}\,\varphi_{y_m}'(y) + \bar{C}\,\varphi_{x_m}'(y) \\ &\varphi_{y_m}''(y) = \bar{E}\, w_m'(y) + \bar{F}\,\varphi_{y_m}(y) + \bar{H}\,\varphi_{x_m}'(y) \\ &\varphi_{x_m}''(y) = \bar{M}\, w_m'(y) + \bar{N}\ \varphi_{y_m}'(y) + \bar{P}\,\varphi_{x_m}(y) \end{aligned} \tag{16}$$

The problem's complexity has caused issues, which have been compounded by the increasing number of variables. Because a differential equation of order n has n number of roots (including repeated roots), we simplify Eq. (15) into n equations of the first order by changing the variables below

$$\begin{aligned} &\varphi_{x_m}(y) = x_1,\ \varphi_{x_m}'(y) = x_2,\quad \varphi''_{x_m}(y) = x_2' = x_3; \\ &\varphi_{y_m}(y) = y_1,\quad \varphi_{y_m}'(y) = y_2,\ \varphi_{y_m}''(y) = y_2' = y_3; \\ &w_m(y) = w_1, w_m'(y) = w_2, w_m''(y) = w_2' = w_3; \\ &x_1' = x_2;\quad x_2' = \bar{M}w_2 + \bar{N}y_2 + \bar{P}x_1 \end{aligned} \tag{17}$$

$$\begin{aligned} &y_1' = y_2;\quad y_2' = \bar{E}w_1 + \bar{F}y_1 + \bar{H}x_2 \\ &w_1' = w_2; w_2' = \bar{A}w_1 + \bar{B}y_1 + \bar{C}x_2 \end{aligned}$$

If we express the system of equations as a product of a matrix in a vector, where Λ is the matrix of coefficients, we consider solutions in the form $\{\xi\}\, e^{ry}$ for this equation, the real roots r and the constant vector $\{\xi\}$ must be determined. For this purpose placing $\{Y\} = \{\xi\}e^{ry}$ in $\{Y'\} = [\Lambda]\{Y\}$ is $r\{\xi\}e^{ry} = [\Lambda]\{\xi\}e^{ry}$. By removing the non-zero scalar statement e^{ry} we have $r\{\xi\} = [\Lambda]\{\xi\}$ or as fallow:

$$([\Lambda] - r[I])\{\xi\} = 0 \tag{18}$$

where I is an (n×n) unit matrix; thus, to resolve the set of differential equations, the above algebraic equations must be solved, and this is precisely the problem of determining the eigenvalues and eigenvectors of the matrix Λ. Therefore, the vector $\{X\}$ is the solution of the equation when r is the eigenvalue of the matrix of coefficients Λ and ξ of the corresponding eigenvector. Now we can put the set of equations into a matrix form as:

$$\begin{bmatrix} -r & 1 & 0 & 0 & 0 & 0 \\ \overline{P} & -r & 0 & \overline{N} & 0 & \overline{M} \\ 0 & 0 & -r & 1 & 0 & 0 \\ 0 & -\overline{H} & \overline{F} & -r & \overline{E} & 0 \\ 0 & 0 & 0 & 0 & -r & 1 \\ 0 & -\overline{C} & \overline{B} & 0 & \overline{A} & -r \end{bmatrix} \begin{bmatrix} \xi_1 \\ \xi_2 \\ \xi_3 \\ \xi_4 \\ \xi_5 \\ \xi_6 \end{bmatrix} = \begin{Bmatrix} 0 \\ 0 \\ 0 \\ 0 \\ 0 \\ 0 \end{Bmatrix} \tag{19}$$

Now, calculating the determinants of the given matrix and setting the result to zero by changing the $r^2 = \mu$:

$$\begin{aligned} &\mu^3 + (-\bar{P} - \bar{F} + \bar{N}\bar{H} + \bar{M}\bar{C} - \bar{A})\mu^2 \\ &+\left(\begin{matrix}\bar{P}\bar{F} - \bar{M}\bar{F}\bar{C} + \bar{N}\bar{E}\bar{C} + \bar{M}\bar{H}\bar{B} \\ -\bar{E}\bar{B} + \bar{P}\bar{A} + \bar{F}\bar{A} - \bar{N}\bar{H}\bar{A}\end{matrix}\right)\mu \\ &+\bar{P}\bar{E}\bar{B} - \bar{P}\bar{F}\bar{A} = 0 \end{aligned} \tag{20}$$

Eq. (20) has three roots μ_1, μ_2, μ_3; by taking the square root of these values, the six real roots of the equation are obtained as $\bar{r}_i\ (i = 1,2,\ldots,6)$, which has three independent values r_1, r_2, r_3, and three dependent values in the form of $-r_1, -r_2, -r_3$. The relationship between $\bar{r}_i$ is defined as $\bar{r}_1 = r_1,\ \bar{r}_2 = -r_1,\ \bar{r}_3 = r_2,\ \bar{r}_4 = -r_2,\ \bar{r}_5 = r_3,\ \bar{r}_6 = -r_3$; So by solving Eq. (19), and assuming $\xi_1 = \hat{A}$ we arrive:

$$\begin{aligned} &\xi_2 = \hat{A}\bar{r}_i;\ \xi_3 = \hat{A}\left(\frac{\bar{r}_i^2 - \bar{P}}{\bar{N}} - \frac{\bar{M}\bar{r}_i}{\bar{N}}\left(\frac{\bar{B}\bar{r}_i^2 - \bar{P}\bar{B} - \bar{C}\bar{N}\bar{r}_i^2}{\bar{N}\bar{r}_i^3 - \bar{N}\bar{A}\bar{r}_i + \bar{M}\bar{r}_i}\right)\right); \\ &\xi_4 = \hat{A}\left(\frac{\bar{r}_i^3 - \bar{P}\bar{r}_i}{\bar{N}} - \frac{\bar{M}\bar{r}_i}{\bar{N}}\left(\frac{\bar{B}\bar{r}_i^2 - \bar{P}\bar{B} - \bar{C}\bar{N}\bar{r}_i^2}{\bar{N}\bar{r}_i^2 - \bar{N}\bar{A} + \bar{M}}\right)\right); \\ &\xi_5 = \hat{A}\left(\frac{\bar{B}\bar{r}_i^2 - \bar{P}\bar{B} - \bar{C}\bar{N}\bar{r}_i^2}{\bar{N}\bar{r}_i^3 - \bar{N}\bar{A}\bar{r}_i + \bar{r}_i\bar{M}}\right);\quad \xi_6 = \hat{A}\left(\frac{\bar{B}\bar{r}_i^2 - \bar{P}\bar{B} - \bar{C}\bar{N}\bar{r}_i^2}{\bar{N}\bar{r}_i^2 - \bar{N}\bar{A} + \bar{M}}\right); \end{aligned} \tag{21}$$

By putting different values of r_i the answer to the Eq. (21) is obtained as follows:

$$Y = \hat{A}_i \begin{bmatrix} 1 \\ \bar{r}_i \\ \left(\frac{\bar{r}_i^2 - \bar{P}}{\bar{N}} - \frac{\bar{M}\bar{r}_i}{\bar{N}}\left(\frac{\bar{B}\bar{r}_i^2 - \bar{P}\bar{B} - \bar{C}\bar{N}\bar{r}_i^2}{\bar{N}\bar{r}_i^3 - \bar{N}\bar{A}\bar{r}_i + \bar{M}\bar{r}_i}\right)\right) \\ \left(\frac{\bar{r}_i^3 - \bar{P}\bar{r}_i}{\bar{N}} - \frac{\bar{M}\bar{r}_i}{\bar{N}}\left(\frac{\bar{B}\bar{r}_i^2 - \bar{P}\bar{B} - \bar{C}\bar{N}\bar{r}_i^2}{\bar{N}\bar{r}_i^2 - \bar{N}\bar{A} + \bar{M}}\right)\right) \\ \left(\frac{\bar{B}\bar{r}_i^2 - \bar{P}\bar{B} - \bar{C}\bar{N}\bar{r}_i^2}{\bar{N}\bar{r}_i^3 - \bar{N}\bar{A}\bar{r}_i + \bar{r}_i\bar{M}}\right) \\ \left(\frac{\bar{B}\bar{r}_i^2 - \bar{P}\bar{B} - \bar{C}\bar{N}\bar{r}_i^2}{\bar{N}\bar{r}_i^2 - \bar{N}\bar{A} + \bar{M}}\right) \end{bmatrix} * e^{-r_i y}; \tag{22}$$

$$i = 1, 2, 3, \dots, 6;$$

Finally, the answer to Eq. (22) is expressed as follows, by using the following variable change to simplify this equation:

$$\hat{A}_i \begin{bmatrix} 1 \\ \bar{r}_i \\ \left(\frac{\bar{r}_i^2 - \bar{P}}{\bar{N}} - \frac{\bar{M}\bar{r}_i}{\bar{N}}\left(\frac{\bar{B}\bar{r}_i^2 - \bar{P}\bar{B} - \bar{C}\bar{N}\bar{r}_i^2}{\bar{N}\bar{r}_i^3 - \bar{N}\bar{A}\bar{r}_i + \bar{M}\bar{r}_i}\right)\right) \\ \left(\frac{\bar{r}_i^3 - \bar{P}\bar{r}_i}{\bar{N}} - \frac{\bar{M}\bar{r}_i}{\bar{N}}\left(\frac{\bar{B}\bar{r}_i^2 - \bar{P}\bar{B} - \bar{C}\bar{N}\bar{r}_i^2}{\bar{N}\bar{r}_i^2 - \bar{N}\bar{A} + \bar{M}}\right)\right) \\ \left(\frac{\bar{B}\bar{r}_i^2 - \bar{P}\bar{B} - \bar{C}\bar{N}\bar{r}_i^2}{\bar{N}\bar{r}_i^3 - \bar{N}\bar{A}\bar{r}_i + \bar{r}_i\bar{M}}\right) \\ \left(\frac{\bar{B}\bar{r}_i^2 - \bar{P}\bar{B} - \bar{C}\bar{N}\bar{r}_i^2}{\bar{N}\bar{r}_i^2 - \bar{N}\bar{A} + \bar{M}}\right) \end{bmatrix} = \begin{bmatrix} \hat{A}_i \\ \bar{B}_i \\ \bar{E}_i \\ \bar{C}_i \\ \bar{F}_i \\ \bar{A}_i \end{bmatrix} \tag{23}$$

$$w_m(y) = \bar{A}_{1_m} e^{-r_{1_m}y} + \bar{A}_{2_m} e^{-r_{2_m}y} + \bar{A}_{3_m} e^{-r_{3_m}y} + \bar{A}_{4_m} e^{-r_{4_m}y} + \bar{A}_{5_m} e^{-r_{5_m}y} + \bar{A}_{6_m} e^{-r_{6_m}y};$$

$$\varphi_{y_m}(y) = \bar{C}_{1_m} e^{-r_{1_m}y} + \bar{C}_{2_m} e^{-r_{2_m}y} + \bar{C}_{3_m} e^{-r_{3_m}y} + \bar{C}_{4_m} e^{-r_{4_m}y} + \bar{C}_{5_m} e^{-r_{5_m}y} + \bar{C}_{6_m} e^{-r_{6_m}y};$$

$$\varphi_{x_m}(y) = \bar{B}_{1_m} e^{-r_{1_m}y} + \bar{B}_{2_m} e^{-r_{2_m}y} + \bar{B}_{3_m} e^{-r_{3_m}y} + \bar{B}_{4_m} e^{-r_{4_m}y} + \bar{B}_{5_m} e^{-r_{5_m}y} + \bar{B}_{6_m} e^{-r_{6_m}y};$$

and can define as:

$$\begin{aligned} w_m(y) &= \bar{A}_{1_m} Cosh(r_{1_m}y) + \bar{A}_{2_m} Sinh(r_{1_m}y) \\ &+ \bar{A}_{3_m} Cosh(r_{2_m}y) + \bar{A}_{4_m} Sinh(r_{2_m}y) \\ &+ \bar{A}_{5_m} Cosh(r_{3_m}y) + \bar{A}_{6_m} Sinh(r_{3_m}y); \end{aligned}$$

$$\begin{aligned} \varphi_{y_m}(y) &= \bar{C}_{1_m} Cosh(r_{1_m}y) + \bar{C}_{2_m} Sinh(r_{1_m}y) \\ &+ \bar{C}_{3_m} Cosh(r_{2_m}y) + \bar{C}_{4_m} Sinh(r_{2_m}y) \\ &+ \bar{C}_{5_m} Cosh(r_{3_m}y) + \bar{C}_{6_m} Sinh(r_{3_m}y); \end{aligned} \tag{24}$$

$$\begin{aligned} \varphi_{x_m}(y) &= \bar{B}_{1_m} Cosh(r_{1_m}y) + \bar{B}_{2_m} Sinh(r_{1_m}y) \\ &+ \bar{B}_{3_m} Cosh(r_{2_m}y) + \bar{B}_{4_m} Sinh(r_{2_m}y) \\ &+ \bar{B}_{5_m} Cosh(r_{3_m}y) + \bar{B}_{6_m} Sinh(r_{3_m}y); \end{aligned}$$

2.4 Extraction of the FG-CNT sandwich plate stiffness matrix

There are three sets of six constants which make up the solutions in Eq. (24), namely, $\bar{A}_{1_m}: \bar{A}_{6_m}$; $\bar{B}_{1_m}: \bar{B}_{6_m}$ and $\bar{C}_{1_m}: \bar{C}_{6_m}$, which are not all independent. First, these unknown coefficients should be specified by applying boundary conditions to extract the stiffness matrix. However, due to the presence of many unknowns in the equations, this is not possible. So, by substituting Eq. (24) into Eq. (14) we can get $\bar{A}_{1_m}$ to $\bar{A}_{6_m}$ and $\bar{C}_{1_m}$ to $\bar{C}_{6_m}$ in terms of $\bar{B}_{1_m}$ to $\bar{B}_{6_m}$:

$$\begin{aligned} &\bar{A}_{1_m} = \delta_1 \bar{B}_{2_m}, \quad \bar{A}_{2_m} = \delta_1 \bar{B}_{1_m}, \quad \bar{A}_{3_m} = \delta_2 \bar{B}_{4_m}, \\ &\bar{A}_{4_m} = \delta_2 \bar{B}_{3_m}, \quad \bar{A}_{5_m} = \delta_3 \bar{B}_{6_m}, \quad \bar{A}_{6_m} = \delta_3 \bar{B}_{5_m} \\ &\bar{C}_{1_m} = \gamma_1 \bar{B}_{2_m}, \quad \bar{C}_{2_m} = \gamma_1 \bar{B}_{1_m}, \quad \bar{C}_{3_m} = \gamma_2 \bar{B}_{4_m} \\ &\bar{C}_{4_m} = \gamma_2 \bar{B}_{3_m}, \quad \bar{C}_{5_m} = \gamma_3 \bar{B}_{6_m}, \quad \bar{C}_{6_m} = \gamma_3 \bar{B}_{5_m}, \end{aligned} \tag{25}$$

where:

$$\begin{aligned} \delta_i = (&-k_s A_{44}\left(k_s A_{55} + r_i{}^2(D_{12} + D_{66})\right) \\ &+ k_s A_{55}(r_i{}^2 D_{22} - \alpha^2 D_{66} + \omega^2 I_2)) \\ &/((r_i k_s A_{44}(k_s A_{55} + r_i{}^2(D_{12} + D_{66})) + r_i(D_{12} \\ &+ D_{66})(-k_s \alpha^2 A_{55} + \omega^2 I_0))); \end{aligned}$$

$$\begin{aligned} \gamma_i = ((&k_s \alpha^2 A_{55} - \omega^2 I_0)(r_i{}^2 D_{22} - \alpha^2 D_{66} + \omega^2 I_2) - \\ &k_s A_{44}(k_s \alpha^2 A_{55} - \omega^2 I_0 + r_i{}^2(r_i{}^2 D_{22} - \alpha^2 D_{66} + \omega^2 I_2)))/ \\ &(r_i \alpha(-k_s A_{44}(k_s A_{55} + r_i{}^2(D_{12} + D_{66})) + (D_{12} + \\ &D_{66})(k_s \alpha^2 A_{55} - \omega^2 I_0))); \end{aligned}$$ with i= 1,2,3.

Consequently, Eq. (24) can be expressed using one group of constants as:

$$\begin{aligned} w_m(y) &= \delta_1 \bar{B}_{2_m} Cosh(r_{1_m}y) + \delta_1 \bar{B}_{1_m} Sinh(r_{1_m}y) \\ &+ \delta_2 \bar{B}_{4_m} Cosh(r_{2_m}y) + \delta_2 \bar{B}_{3_m} Sinh(r_{2_m}y) \\ &+ \delta_3 \bar{B}_{6_m} Cosh(r_{3_m}y) + \delta_3 \bar{B}_{5_m} Sinh(r_{3_m}y) \\ \varphi_{y_m}(y) &= \bar{B}_{1_m} Cosh(r_{1_m}y) + \bar{B}_{2_m} Sinh(r_{1_m}y) \\ &+ \bar{B}_{3_m} Cosh(r_{2_m}y) + \bar{B}_{4_m} Sinh(r_{2_m}y) \\ &+ \bar{B}_{5_m} Cosh(r_{3_m}y) + \bar{B}_{6_m} Sinh(r_{3_m}y) \\ \varphi_{x_m}(y) &= \gamma_1 \bar{B}_{2_m} Cosh(r_{1_m}y) + \gamma_1 \bar{B}_{1_m} Sinh(r_{1_m}y) \\ &+ \gamma_2 \bar{B}_{4_m} Cosh(r_{2_m}y) + \gamma_2 \bar{B}_{3_m} Sinh(r_{2_m}y) \\ &+ \gamma_3 \bar{B}_{6_m} Cosh(r_{3_m}y) + \gamma_3 \bar{B}_{5_m} Sinh(r_{3_m}y) \end{aligned} \tag{26}$$

Inserting Eq. (26) into Eqs. (9)-(10), gives us the values of forces and moments as:

$$\begin{aligned} Q_{y_m} = k_s A_{55} (&\bar{B}_{1_m}(1 + r_{1_m}\delta_1)\, Cosh(r_{1_m}y) \\ &+ \bar{B}_{2_m}(1 + r_{1_m}\delta_1)\, Sinh(r_{1_m}y) \\ &+ \bar{B}_{3_m}(1 + r_{2_m}\delta_2) Cosh(r_{2_m}y) \\ &+ \bar{B}_{4_m}(1 + r_{2_m}\delta_2)\, Sinh(r_{2_m}y) \\ &+ \bar{B}_{5_m}(1 + r_{3_m}\delta_3) Cosh(r_{3_m}y) \\ &+ \bar{B}_{6_m}(1 + r_{3_m}\delta_3)\, Sinh(r_{3_m}y)\,) \end{aligned}$$

$$\begin{aligned} M_y = Sin(\alpha x)(&\bar{B}_{1_m}(D_{22} r_{1_m} + D_{12}\alpha\gamma_1) Sinh(r_{1_m}y) \\ &+ \bar{B}_{2_m}(D_{22} r_{1_m} + D_{12}\alpha\gamma_1) Cosh(r_{1_m}y) \\ &+ \bar{B}_{3_m}(D_{22} r_{2_m} + D_{12}\alpha\gamma_2) Sinh(r_{2_m}y) \\ &+ \bar{B}_{4_m}(D_{22} r_{2_m} + D_{12}\alpha\gamma_2) Cosh(r_{2_m}y) \\ &+ \bar{B}_{5_m}(D_{22} r_{3_m} + D_{12}\alpha\gamma_3) Sinh(r_{3_m}y) \\ &+ \bar{B}_{6_m}(D_{22} r_{3_m} + D_{12}\alpha\gamma_3) Cosh(r_{3_m}y)) \end{aligned} \tag{27}$$

$$\begin{aligned} M_{xy} = -D_{66}(&\bar{B}_{1_m}(\alpha - \gamma_1 r_{1_m}) Cosh(r_{1_m}y) \\ &+ \bar{B}_{2_m}(\alpha - \gamma_1 r_{1_m}) Sinh(r_{1_m}y) \\ &+ \bar{B}_{3_m}(\alpha - \gamma_2 r_{2_m}) Cosh(r_{2_m}y) \\ &+ \bar{B}_{4_m}(\alpha - \gamma_2 r_{2_m}) Sinh(r_{2_m}y) \\ &+ \bar{B}_{5_m}(\alpha - \gamma_3 r_{3_m}) Cosh(r_{3_m}y) \\ &+ \bar{B}_{6_m}(\alpha - \gamma_3 r_{3_m}) Sinh(r_{3_m}y)) \end{aligned}$$

According to Fig. 4, force and displacement boundary conditions must be taken into account for the sandwich plate.

Boundary conditions for the displacements and rotations:

$$\begin{aligned} &At\ y = -\frac{b}{2}: w_m = w_1,\ \varphi_{x_m} = \varphi_{x_1},\ \varphi_{y_m} = \varphi_{y_1} \\ &At\ y = b/2:\ w_m = w_2,\ \varphi_{x_m} = \varphi_{x_2},\ \varphi_{y_m} = \varphi_{y_2} \end{aligned} \tag{28}$$

similarly, force boundary conditions are:

$$\begin{aligned} &At\ y = -b/2: Q_{x_m} = -Q_{y1}, M_{x_m} = -M_{y_1}, M_{xy_m} = -M_{xy_1} \\ &At\ y = b/2: Q_{x_m} = Q_{y2},\ M_{x_m} = M_{y_2},\ M_{xy_m} = M_{xy_2} \end{aligned} \tag{29}$$

Now, by substituting the conditions of Eq. (28) in Eq. (26), the following matrix is achieved with regards to the displacements.

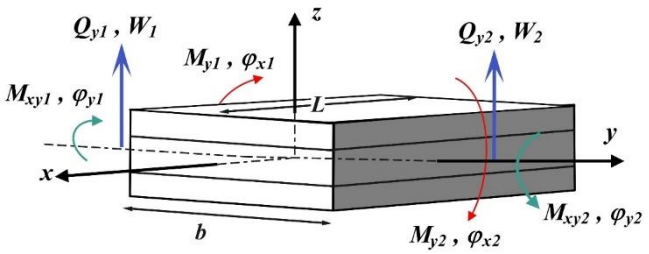

Fig. 4 Edge conditions of the sandwich plate strip and sign conventions

$$\begin{bmatrix} W_1 \\ \varphi_{x_1} \\ \varphi_{y_1} \\ W_2 \\ \varphi_{x_2} \\ \varphi_{y_2} \end{bmatrix} = \begin{bmatrix} 0 & \delta_1 & 0 & \delta_2 & 0 & \delta_3 \\ 1 & 0 & 1 & 0 & 1 & 0 \\ 0 & \gamma_1 & 0 & \gamma_2 & 0 & \gamma_3 \\ \delta_1 S_{h_1} & \delta_1 C_{h_1} & \delta_2 S_{h_2} & \delta_2 C_{h_2} & \delta_3 S_{h_3} & \delta_3 C_{h_3} \\ C_{h_1} & S_{h_1} & C_{h_2} & S_{h_2} & C_{h_3} & S_{h_3} \\ \gamma_1 S_{h_1} & \gamma_1 C_{h_1} & \gamma_2 S_{h_2} & \gamma_2 C_{h_2} & \gamma_3 S_{h_3} & \gamma_3 C_{h_3} \end{bmatrix} \begin{bmatrix} \bar{B}_1 \\ \bar{B}_2 \\ \bar{B}_3 \\ \bar{B}_4 \\ \bar{B}_5 \\ \bar{B}_6 \end{bmatrix} \quad (30)$$

By substituting the boundary conditions for forces and moments, Eq. (29) in Eq. (27), and rewrite it in the form of a matrix as:

$$\begin{bmatrix} Q_{y1} \\ M_{y1} \\ M_{xy1} \\ Q_{y2} \\ M_{y2} \\ M_{xy2} \end{bmatrix} = \begin{bmatrix} -L_1 & 0 & -L_2 & 0 & -L_3 & 0 \\ 0 & -R_1 & 0 & -R_2 & 0 & -R_3 \\ -T_1 & 0 & -T_2 & 0 & -T_3 & 0 \\ L_1 C_{h_1} & L_1 S_{h_1} & L_2 C_{h_2} & L_2 S_{h_2} & L_3 C_{h_3} & L_3 S_{h_3} \\ R_1 S_{h_1} & R_1 C_{h_1} & R_2 S_{h_2} & R_2 C_{h_2} & R_3 S_{h_3} & R_3 C_{h_3} \\ T_1 C_{h_1} & T_1 S_{h_1} & T_2 C_{h_2} & T_2 S_{h_2} & T_3 C_{h_3} & T_3 S_{h_3} \end{bmatrix} \begin{bmatrix} \bar{B}_1 \\ \bar{B}_2 \\ \bar{B}_3 \\ \bar{B}_4 \\ \bar{B}_5 \\ \bar{B}_6 \end{bmatrix} \quad (31)$$

In the above equations, we have used the following simplified expressions:

$$T_i = D_{66}(\alpha - \gamma_i r_i), \qquad R_i = D_{12}\,\alpha\,\gamma_i + D_{11} r_i,$$
$$L_i = k_s A_{55}(\delta_i r_i + 1), \qquad C_{h_i} = Cosh(r_i b),$$
$$S_{h_i} = Sinh(r_i b); \quad i = 1,2,3.$$

Eq. (30) can be expressed in the general form $\{\delta\} = [V]\{B\}$, and Eq. (31) can be expressed in the general form $\{F\} = [R]\{B\}$. Since force is equal to the product of stiffness in displacement ($\{F\} = [K]\{\delta\}$), then we can calculate the stiffness matrix with the following expression:

$$K = RV^{-1} \quad (32)$$

Sometimes the support conditions of the sandwich plate on the two side ($x = -\mathrm{L}/2$ and $x = L/2$) should be SS. The other two sides of the strips can have any support conditions (see Fig. 4). The FSM assembly system is analogous to the finite element technique. It is noteworthy that each strip of the sandwich plate is linked through nodal lines instead of singular points. Penalty approach are commonly employed to restrict a particular degree of freedom. This approach involves increasing the rigidity of the pertinent coefficient on the primary diagonal of the dynamic stiffness matrix. Note the general approach as follows:

• Formulate the stiffness matrix of each strip.

• Write the strips in global displacement relations.

• Assemble the global stiffness matrix. Each strip stiffness matrix has been added to the location in the global stiffness matrix corresponding to the identical degree of freedom related to the strip.

• Reduce the global stiffness matrix component in conformity with given constraints.

• Solve the governing equations for the indeterminate strip displacements.

• Solve the equations by back substitution to compute the reaction forces.

Therefore, at the study's beginning, determine each strip's stiffness matrix and then calculate the reduced global stiffness matrix, represented as non-algebraic functions of the problem parameters, including in-plane forces and natural frequencies. We can set the determinants of the global stiffness matrix equal to zero to compute the natural frequency as:

$$Det[K(\omega)] = 0 \quad (33)$$

So, by putting the specific values of the in-plane forces of the sandwich plate in Eq. (33), the natural frequency (ω) is obtained. Coefficients of the finite strip stiffness matrix are provided in Explicit expressions. Due to the complexity of these coefficients, using a developed computational program such as Mathematica (Wolfram and Gray 2022) is essential. To ward off numerical unstableness and overflows, the expressions must be simplified and arranged. The entire simplification is accomplished by applying the explicit expressions of the terms included in the matrix V and R (Eqs. (30) and (31)). It is not advised to invert the matrix V, as it may lead to undesirable conditions. Following simplifications, the finite strip stiffness matrix can be generated, causing no numerical error using the explicit terms. For this purpose, in the Mathematica, We can draw the logarithm of the determination of the absolute value of the stiffness matrix (Log[Abs[Det[K]]]) in terms of vibration frequency. In this diagram, we can calculate the approximate values of the frequency (vertical asymptotes of the diagram). Then, the exact values can be calculated using numerical methods.

3. Results and discussion

The complete process starting from forming the global stiffness matrix of the single and multi-span FG-CNT sandwich plate and finishing with calculating natural frequencies has been implemented in a computer program using Mathematica. The sandwich plate is divided into a few strips in the exact finite strip method. The shape functions for the transverse direction are assumed to be the same trigonometric terms for every boundary condition in the y direction. On the other hand, in the longitudinal direction, exponential functions are taken. The functions need to abide by the pre-set boundary conditions and the differential equation of motion of the sandwich plate. By defining displacement vectors and nodal lines forces, each finite strip's exact stiffness matrix is extracted as a function of free vibration frequencies. By forming the stiffness matrix of the whole sandwich plate, it is possible to calculate the exact free vibration frequencies of these FG-CNT sandwich plates. This article's method and theory presented herein are first validated against exact results in the literature for FG-CNT sandwich plates with various boundary conditions as Fig. 5. Once the results have been

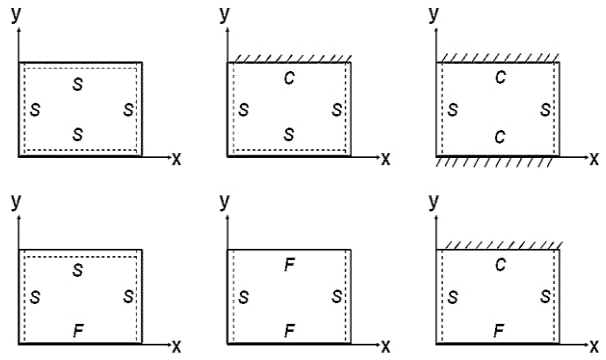

Fig. 5 Boundary conditions of the FG-CNT sandwich plate

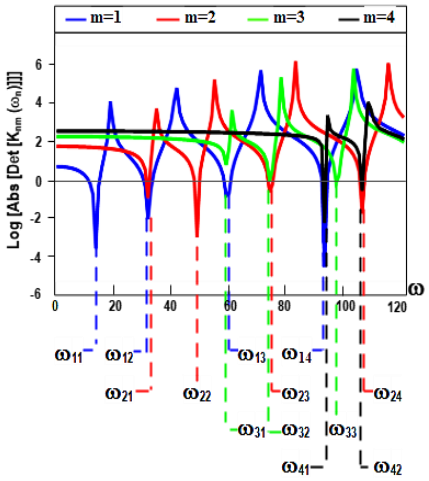

(a) SSSS

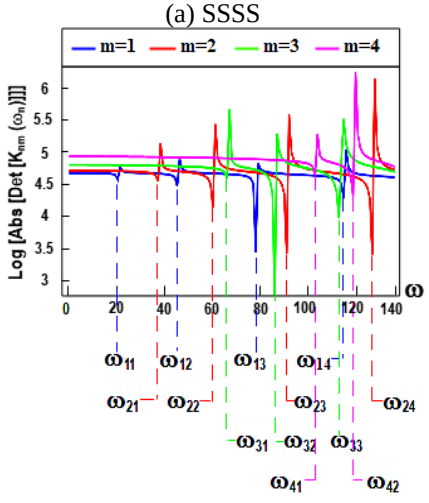

(b) SCSC

Fig. 6 Natural frequencies of a square isotropic plate for boundary condition

verified, multiple examples are demonstrated to prove the ability of the devised procedure to solve a variety of issues, for instance, the length-to-thickness ratio and the face sheet-to-core thickness of the single and multi-span FG-CNT sandwich plates with diverse boundary conditions.

3.1 Validation of free vibration analysis

This section checks the validity of the extracted equations for calculating the vibration frequency of an FG-CNT sandwich plate with simple boundary conditions on four sides (SSSS). To begin, FSDT with SSSS boundary conditions is used to calculated the exact frequencies of the free transverse vibration of isotropic square plates, which are compared with the research result (Malik and Bert 1998, Reddy 2003, Zenkour 2005, Boscolo and Banerjee 2011). For this purpose, an isotropic square plate with the parametric study of $L = 10\ h, \nu = 0.3$ are investigated.

The components of the stiffness matrix are transcendental functions that are related to the eigenvalues. A trial-and-error method is essential to gain natural frequencies from the eigenfunction of the FG-CNT sandwich plate expressed in Eq. (33). Fig. 6 provides a visual representation of the plate's free vibration parameter ($Det[K(\omega_{mn})]$) displayed on a logarithmic scale. The natural frequencies are the points along the horizontal axis where the logarithmic function tends to negative infinity. The coefficient m in ω_{mn} is expressing the number of half-wavelengths in the x-direction. The coefficient n is the root number within the characteristic function expressed in Eq. (33). Fig. 6(a), exemplifies that the first and second natural frequencies for the SSSS boundary condition can be calculated by a one-half wave in the plate width (m =1). The third frequency is related to a double wave with a magnitude of m = 2. These exact frequency values are: $\omega_{11} = 13.1561$, $\omega_{12} = 31.3861$ and $\omega_{22} = 48.1626$, and the Non-dimensionless natural frequencies $\bar{\omega}_{mn} = \omega\,(L^2/h)\sqrt{\rho/E}$ are given in the last column of Table 1. Similarly, in Fig. 6(b) it is shown for the SCSC boundary condition, and the Nondimensionalized natural frequencies are given in the last column of Table 2. With these examples, we can understand how to extract results from mathematical software.

Table 2 provides a comparison between the natural frequency parameters and the exact solution from Boscolo and Banerjee (2011) which is derived from FSDT for SCSC boundary conditions.

As presented in Tables 1-2, The findings of the current theories are in well agreement with the analytical results of the research literature (Malik and Bert 1998, Reddy 2003, Zenkour 2005, Boscolo and Banerjee 2011) for the square isotropic plate.

Next, we have validated the natural frequencies of FG-CNT sandwich plates of the present FSDT against different theories (Zenkour 2005, Li *et al.* 2008, Meiche *et al.* 2011, Thai *et al.* 2014) in Table 3. This table presents the natural frequencies of FG-CNT sandwich plates with six lay-up schemes and different values of the volume fraction exponent (p). The material properties (Zenkour 2005) are considered to be:

$$E_f = 70\ E_0,\ \nu_f = 0.3,\ \rho_f = 27070\ \rho_0\ (for\ face\ sheet)$$
$$E_c = 380\ E_0,\ \nu_c = 0.3,\ \rho_c = 38000\ \rho_0\ (for\ core)$$

where $E_0 = 1\ GPa\ and\ \rho_0 = 1\ N/m^3$. The sheer correction factor (k_s), in FSDPT is set to a value of $5/6$. The outcomes are illustrated in terms of non-dimensional natural frequencies (as $\bar{\omega}_{mn} = \omega\,(L^2/h)\sqrt{\rho_0/E_0}$). Table 3 shows that there is a great deal of agreement between the present solution and other theories. As it is observed, the frequencies decrease alongside the rise in p. Additionally,

Table 1 Free vibration analysis of the simply supported square isotropic plates with the SSSS boundary condition, $L = 10h,\ \nu = 0.3$, and k_s=5/6

m	n	FSDPT (Reddy 2003)	FSDPT (Zenkour 2005)	CLPT (Zenkour 2005)	TSDPT (Zenkour 2005)	DQM (Malik and Bert 1998)	FSDPT (Boscolo and Banerjee 2011)	Present Study
1	1	5.76901	5.76932	5.92483	5.76941	5.77692	5.76949	5.76932
1	2	13.76401	13.76275	14.63551	13.76403	13.80502	13.76350	13.76370
2	2	21.12109	21.11383	23.14416	21.11839	21.21445	21.12052	21.12071
1	3	25.73403	25.71663	28.70950	25.72431	25.86979	25.73346	25.73371
2	3	32.28409	32.25169	36.90402	32.25169	32.49153	32.28390	32.28392
1	4	40.43606	40.31266	47.55756	40.33980	40.74998	40.43587	40.43563

Classical Laminated Plate Theory, FSDPT: First-order Shear Deformation Plate Theory, TSDPT: Trigonometric Shear Deformation Plate Theory, and DQM: Differential Quadrature Method.

Table 2 Nondimensionalized natural frequencies of the SCSC square isotropic plates, $\bar{\omega}_{mn} = \omega\,(L^2/h)\sqrt{\rho/E}$, $L = 10h,\ \nu = 0.3$, and $k_s = 5/6$

Mode (m,n)	CPT (Boscolo and Banerjee 2011)	FSDT (Boscolo and Banerjee 2011)	FSDT Present Study
(1,1)	28.9508	26.6683	26.6120
(2,1)	54.7431	49.1129	48.9768
(1,2)	69.3270	59.2102	59.0827
(2,2)	94.5853	78.8130	78.4389
(3,1)	102.216	86.8440	86.6756
(1,3)	129.095	101.371	101.183
(3,2)	140.204	112.058	111.526
(2,3)	154.775	118.922	118.338
(4,1)	170.346	134.595	134.430
(3,3)	199.810	148.316	147.421
(1,4)	206.697	149.990	149.763
(4,2)	208.391	155.788	155.225

when the thickness of the core decreases, the natural frequencies decrease.

Now, by examining the results of Tables 1-3, we can confirm the accuracy of the new formulation for all types of boundary conditions of the FG-CNT sandwich plates. Furthermore, the FG-CNT sandwich plate formulation can be developed to accommodate different boundary conditions and the calculation of any exact natural frequencies with a desired level of accuracy.

3.2 Parametric study

Confirming the validation we obtained in the previous section, several FG-CNT sandwich plates are analysed using the new formulation of the exact finite strip method with the FSDT. To make the results uniform and comparable, most numerical results are presented in dimensionless form. To create comparable and uniform results, most numerical findings are expressed as the dimensionless natural frequencies ($\bar{\omega}_{mn} = \omega\,(L^2/h)\sqrt{\rho_0/E_0}$). The parametric studies are conducted in the following section to investigate the influence of geometric parameters on the natural frequencies of the FG- CNT sandwich plates. The same material properties as those presented in the previous section are given. First, the following parameters are investigated: $L = b; L/h = 10; p = 2,$ and $k_s = 2/3, 5/6$ and 1. The free vibration analysis results of two lay-up schemes 1-2-1 and 2-2-1 are shown in Table 4.

Table 4 provides comparisons based on symmetrical (1-2-1) against non-symmetrical (2-2-1) sandwich plates. As the mode number rises, the frequencies become higher. The shear correction factor decreases the frequency. Table 4 shows that when the k_s is decreased, the frequencies decrease as well. Consequently, we have taken the mid-range value for the shear correction factor ($k_s = 5/6$), which is neither a higher nor a lower value. This example illustrates the precision and effectiveness of the present technique in the free vibration analysis of FG-CNT sandwich plates with various boundary conditions, as shown in Fig. 5, and various

length-to-thickness ratios (L/h) with different volume fraction exponents (p). The natural frequency results are listed in Table 5.

According to Table 5, it can be seen that in different boundary conditions, with the increase of the L/h ratio, the value of non-dimensional natural frequency ($\bar{\omega}$)

Table 3 Free vibration analysis of the simply supported square isotropic plates with different lay-up schemes, and volume fraction exponent (p)

Lay-up	p	CLPT (Zenkour 2005)	HSDT (Meiche *et al.* 2011)	3D (Li *et al.* 2008)	FSDPT (Zenkour 2005)	FSDPT (Thai *et al.* 2014)	Present Study
1-0-1	0	1.87359	1.82450	1.82680	1.82442	1.82440	1.82442
	0.5	1.47157	1.44420	1.44610	1.44168	1.44420	1.44168
	1	1.26238	1.24310	1.24470	1.24031	1.24290	1.24032
	5	0.95844	0.94570	0.94480	0.94256	0.94310	0.94256
2-1-2	0	1.87359	1.82450	1.82680	1.82442	1.82440	1.82442
	0.5	1.51242	1.48410	1.48610	1.48159	1.48410	1.48159
	1	1.32023	1.30000	1.30180	1.29729	1.30000	1.29729
	5	0.99190	0.98170	0.98100	0.97870	0.97960	0.97870
1-1-1	0	1.87359	1.82450	1.82680	1.82442	1.82440	1.82442
	0.5	1.54903	1.51920	1.52130	1.51695	1.51920	1.51695
	1	1.37521	1.35330	1.35520	1.35072	1.35330	1.35072
	5	1.05565	1.04460	1.04530	1.04183	1.04350	1.04183
2-2-1	0	1.87359	1.82450	1.82680	1.82442	1.82440	1.82442
	0.5	1.58374	1.54710	1.54930	1.55001	1.54710	1.55001
	1	1.43247	1.39560	1.39760	1.40555	1.39560	1.40555
	5	1.16195	1.10880	1.10980	1.14467	1.10770	1.14467
1-2-1	0	1.87359	1.82450	1.82680	1.82442	1.82440	1.82442
	0.5	1.60722	1.57460	1.57670	1.57274	1.57450	1.57274
	1	1.46497	1.43940	1.44140	1.43722	1.43930	1.43722
	5	1.18867	1.17400	1.17570	1.17159	1.17350	1.17159

Table 4 The first 10 natural frequency of 1-2-1 and 2-2-1 lay-up schemes of the FGM sandwich plates ($\bar{\omega}_{mn} = \omega(L^2/h)\sqrt{\rho_0/E_0}$) with various shear correction factor (k_s)

m	n	lay-up scheme					
		1-2-1			2-2-1		
		k_s=2/3	k_s=5/6	k_s=1	k_s=2/3	k_s=5/6	k_s=1
1	1	1.294909	1.300199	1.303759	1.260090	1.265240	1.268710
1	2	3.115390	3.144590	3.164500	3.031309	3.059759	3.079150
2	2	4.813950	4.880839	4.926909	4.683629	4.748770	4.793640
1	3	5.888899	5.986509	6.054130	5.729209	5.824250	5.890109
2	3	7.426720	7.577009	7.681720	7.225179	7.371190	7.473139
1	4	9.358339	9.586849	9.747770	9.103390	9.325799	9.482420
3	3	9.821900	10.071650	10.247400	9.554590	9.797249	9.968460
2	4	10.729820	11.021940	11.228809	10.437079	10.721340	10.922640
3	4	12.891110	13.295409	13.584009	12.538659	12.931999	13.212760
4	4	15.698579	16.268189	16.678530	15.268380	15.822419	16.221510

increases, which is also true in higher volume fraction exponent (p). Also, the natural frequencies decrease as the p increases. As expected, in the free boundary condition, we have a lower $\bar{\omega}$ against simple and clamped boundary conditions. Therefore, in this article, the lowest value of $\bar{\omega}$ occurred in the SFSF boundary condition, and the highest value occurred in the SCSC boundary condition.

Table 6 shows the effect of lay-up schemes on the natural frequencies of FG-CNT sandwich plates with different length-to-thickness ratios (L/h), where the power-law index is taken to be $p = 5$. In addition, the variation in the dimensionless vibration frequencies of these sandwich plates with different lay-up schemes versus (L/h), is shown in Fig. 7. As the results indicate, the 1-2-1 lay-up scheme gives the highest natural frequency and the 1-0-1 shows the lowest value for the types of FG-CNT sandwich plates considered. Therefore, by increasing the proportion of the thickness of the core within the value of the total thickness

Table 5 Dimensionless natural frequencies calculation for the (1-2-1) FGM sandwich plate $\bar{\omega}_{mn} = \omega(L^2/h)\sqrt{\rho_0/E_0}$ with different boundary conditions, $L = b$

p	L/h	Boundary conditions					
		SFSF	SFSS	SFSC	SSSS	SSSC	SCSC
0	0.01	0.00562421	0.00628809	0.00628808	0.00616148	0.00688868	0.00871343
	0.05	0.02810420	0.03142535	0.03142435	0.03084480	0.03447685	0.04359364
	0.1	0.05610359	0.06275680	0.06274869	0.06192304	0.06916259	0.08735250
	0.5	0.26574000	0.30024000	0.29973945	0.34487500	0.38462450	0.38256345
	5	0.88363025	1.08811485	1.17170500	1.66974000	1.87654950	2.11805525
2	0.01	0.00504689	0.00514409	0.00564262	0.00460109	0.00514409	0.00650666
	0.05	0.02520450	0.02576095	0.02818265	0.02305070	0.02576095	0.03256530
	0.1	0.05022449	0.05177420	0.05617810	0.04638323	0.05177420	0.06533039
	0.5	0.22852450	0.25986497	0.25882354	0.27319400	0.29641845	0.32878746
	5	0.63568950	0.78614950	0.85460950	1.22020950	1.39806525	1.61477500
5	0.01	0.00487042	0.00466178	0.00544531	0.00416970	0.00466178	0.00589657
	0.05	0.02431525	0.02335120	0.02718740	0.02089580	0.02335119	0.02951630
	0.1	0.04840490	0.04696569	0.05413660	0.04208560	0.04696569	0.05924110
	0.5	0.21645900	0.24672850	0.24543095	0.25300103	0.27363100	0.31006399
	5	0.57397455	0.71048985	0.77410950	1.10559449	1.27275000	1.47873000
10	0.01	0.00478473	0.00446339	0.00534950	0.00399225	0.00446339	0.00564562
	0.05	0.02388350	0.02235970	0.02670375	0.02000910	0.02235970	0.02826190
	0.1	0.04752200	0.04498569	0.05314320	0.04031547	0.04498569	0.05673010
	0.5	0.21089395	0.24061595	0.23920800	0.24441995	0.26400845	0.30130045
	5	0.54941450	0.68031450	0.74183450	1.05958450	1.22188500	1.42271950

Table 6 Dimensionless natural frequencies calculation for the FGM sandwich plate, $p = 5$, SSSS, with different lay-up schemes and L/h ratio

L/h	lay-up scheme					
	1-2-1	2-1-2	2-2-1	1-0-1	2-1-1	1-1-1
0.1	0.0420856	0.0347099	0.0407992	0.0326927	0.0378533	0.0373048
0.5	0.2530010	0.2111760	0.2439570	0.1924010	0.2258500	0.2276250
1	0.5647610	0.4808701	0.5457681	0.4337959	0.5082427	0.5150260
2	0.8512026	0.7182440	0.8263140	0.6662118	0.7709860	0.7674470
3	0.9910950	0.8327820	0.9645960	0.7841010	0.9011340	0.8885380
4	1.0642276	0.8921660	1.0372700	0.8472600	0.9709040	0.9510760
7	1.1470194	0.9589780	1.1198200	0.9204440	1.0481513	1.0211900
10	1.1715890	0.9787006	1.1446690	0.9425612	1.0715600	1.0418348
14	1.1838680	0.9885430	1.1570200	0.9536950	1.0833000	1.0521300
20	1.1905960	0.9939310	1.1637900	0.9598190	1.0897400	1.0577600

of the sandwich plate, the natural frequencies have increased in any lay-up schemes, and as the plates become thinner (the L/h ratio increases).

The dimensionless natural frequencies of 1-2-1, 2-1-2, and 2-2-1 lay-up of the FG-CNT sandwich plate with SSSS boundary conditions, are listed in Table 7 with various power-law index (p) and (L/h) ratios. With an increase in the core component of the functionally graded sandwich plate, the exponent of the volume fraction decreases. However, the vibration frequencies increase. Moreover, the highest natural frequency given from the 1-2-1 lay-up scheme, as the (L/h) ratio increases.

Fig. 8 indicates the variation of the dimensionless fundamental frequency of a FG-CNT sandwich plate with SSSS boundaries according to several power-law indices and length-to-thickness ratios for various layup schemes. It is clear that the value of the dimensionless natural frequency ($\bar{\omega}$) decreases as the exponent of the volume

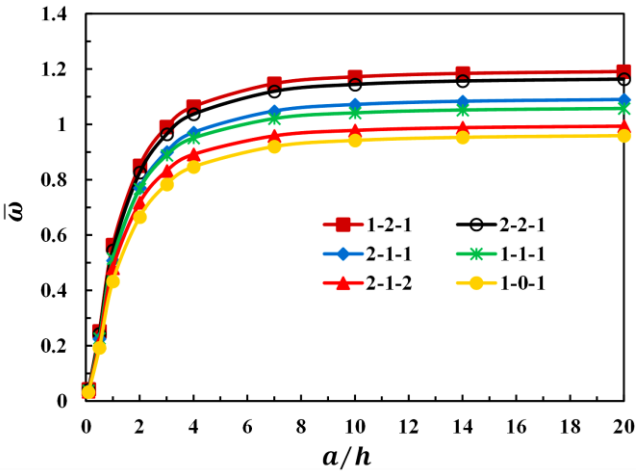

Fig. 7 Natural frequencies of the square FG-CNT sandwich plate with different lay-up schemes for SSSS boundary condition

Table 7 The effect of lay-up schemes 1-2-1, 2-1-2 and 2-2-1 of the SSSS FGM sandwich plate, with different power-law index (p)

L/h	p	lay-up scheme		
		2-1-2	1-2-1	2-2-1
0.1	0	0.06192304	0.06192304	0.06192300
	1	0.04591989	0.05074385	0.04957969
	2	0.03984101	0.04638323	0.04498179
	5	0.03470990	0.04208560	0.04079919
	10	0.03314449	0.04031547	0.03925401
1	0	0.71652390	0.71652390	0.71652390
	1	0.58967303	0.63516990	0.62268900
	2	0.53500940	0.60116490	0.58448190
	5	0.48087008	0.56476100	0.54576806
	10	0.45988040	0.54847200	0.52952490
10	0	1.82441970	1.82441970	1.82441970
	1	1.29728899	1.43722440	1.40554898
	2	1.11947000	1.30019900	1.26524000
	5	0.97870060	1.17158898	1.14466898
	10	0.93961920	1.12066898	1.10261430

fraction (p) increases for the L/h ratios. Because raising the power-law index reduces the stiffness of the FG-CNT sandwich plate.

3.3 Free vibration analysis of the multi-span FG-CNT sandwich plate

In this part of the study, an exploration of the free vibration of sandwich plates across multiple spans was conducted. Rectangular FG-CNT sandwich plates with middle support (as shown in Fig. 9) are structures that have many uses in engineering. This plate can be used in bridges, buildings, and aerospace and mining engineering. Practically, internal support lines are used to reduce static and dynamic

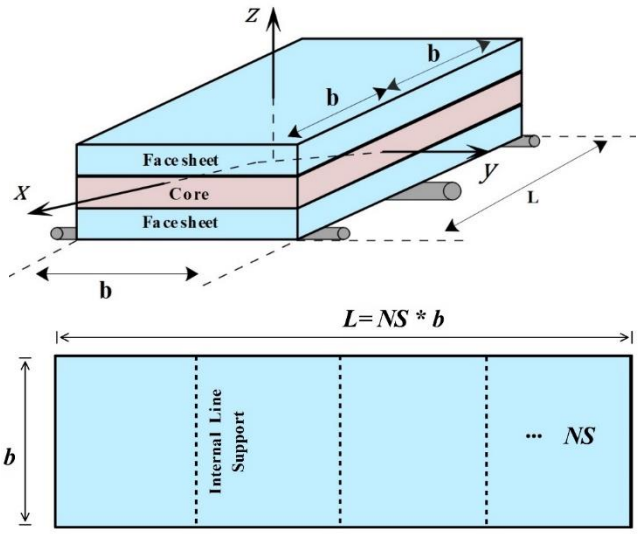

Fig. 9 The FG-CNT Sandwich plate with interior line support (NS: the Number of Span)

Table 8 Dimensionless natural frequencies calculation for the FGM sandwich plate, $p = 5$, SSSS, with different lay-up schemes and L/h ratio

NS	lay-up scheme			
	$p = 0$	$p = 1$	$p = 2$	$p = 5$
	2-1-2			
1	1.824420	1.297289	1.119470	0.978701
2	1.154789	0.907054	0.819784	0.738092
3	1.028939	0.807749	0.729904	0.657062
4	0.984743	0.772909	0.698372	0.628649
	1-2-1			
1	1.824420	1.437224	1.300199	1.171589
2	1.154789	0.818254	0.705389	0.616376
3	1.028939	0.728588	0.627976	0.548674
4	0.984743	0.697133	0.600825	0.524935

stresses and displacements of the structure or satisfaction some architectural requirements used in the structures (Hosseini-Hashemi *et al.* 2009). It should be noted that these supports only prevent movement in the vertical direction. Boundary conditions in a multi-span FG-CNT sandwich plate mean boundary conditions on four sides of the structure. Also, the internal line support is placed parallel to the simple supports. In this paper, the length value is a coefficient of the width of the FG-CNT sandwich plate, so the number of span (NS) is a natural number. The free vibration analysis results are given in Table 8.

Through examining the data in Table 8, clear that the vibration frequency of the FG-CNT sandwich plate decreases as the span (line of boundary condition) increases, which means increasing the rigidity of supports. Furthermore, the natural frequencies decrease as the p increases. Consequently, the natural frequencies of multi-span FG-CNT sandwich plates are decreased as the number of spans (NS) increases.

4. Conclusions

This paper analysed the exact finite strip method. The first-order shear deformation theory was then used to further expand upon the theory in order to work out the free vibration frequency of functionally graded-carbon nanotube (FG-CNT) sandwich plates with a variety of boundary conditions. The global stiffness matrix of the single and multi-span FG-CNT sandwich plate has been computationally evaluated, leading to the calculation of the natural frequencies, using a computer program created with Mathematica. In the validation section, the finite strip method with first-order shear theory has a very high accuracy compared to the literature research. An essential benefit of the finite strip method is its proficiency when dealing with many boundary conditions. A comprehensive parametric investigation was performed on the non-dimensional frequency of the FG-CNT sandwich plate, varying parameters such as the length-to-thickness ratio, power-law index, and layup schemes of single and multi-span sandwich plates with distinct boundary conditions. By the way, the results obtained in this research are stated as follows:

• In the exact finite strip method, shape functions are the governing equation's analytical answer, which leads to a detailed analysis of the sandwich plate problem based on the selected theory. Of course, it is evident that the extraction of natural frequencies, which are obtained from complex equations, requires a numerical method that can increase the accuracy of this method. According to these explanations, this method is more accurate compared to the methods that use approximate shape functions.

• The overall solution exactly fulfills the governing equation of the eigenvalue issue. Some capabilities of this method include modeling the different boundary conditions, as well as modeling the intermediate rollers.

• When the ratio of the core thickness to the total thickness of the structure increases, the natural frequencies increase.

• As the results indicate, the 1-2-1 lay-up scheme gives the highest natural frequency and the 1-0-1 shows the lowest value for the types of FG-CNT sandwich plates considered.

• The value of the dimensionless natural frequency ($\bar{\omega}$) decreases as the exponent of the volume fraction (p) increases.

• In different boundary conditions, with the increase of the L/h ratio, the value of non-dimensional natural frequency ($\bar{\omega}$) increases.

• The new exact results are expected to provide other researchers with data to compare their results against.

• The finite strip method has yielded exact results with great precision and accuracy, which can assess the reliability and accuracy of other numerical approaches. It is proposed that higher-order theories be used to estimate the frequencies of the FG-CNT sandwich plate.

References

Bahrami, M.R. and Hatami, S. (2016), "Free and forced transverse vibration analysis of moderately thick orthotropic plates using spectral finite element method", *J. Solid Mech.*, **8**(4), 895-915. https://doi.org/20.1001.1.20083505.2016.8.4.15.9.

Barati, A., Hadi, A., Nejad, M.Z. and Noroozi, R. (2022), "On vibration of bi-directional functionally graded nanobeams under magnetic field", *Mech. Based Des Struct. Mach.*, **50**(2), 468-485. https://doi.org/10.1080/15397734.2020.1719507.

Boscolo, M. and Banerjee, J.R. (2011), "Dynamic stiffness elements and their applications for plates using first order shear deformation theory", *Comput. Struct.*, **89**(3-4), 395-410. https://doi.org/10.1016/j.compstruc.2010.11.005.

Cheung, Y.K. (1968), "The finite strip method in the analys of elastic plates with two opposite simply supported ends", *Proceedings of the Institution of Civil Engineers*, **40**(1), 1-7.

Chiker, Y., Bachene, M., Attaf, B., Hafaifa, A. and Guemana, M. (2023), "Uncertainty influence of nanofiller dispersibilities on the free vibration behavior of multi-layered functionally graded carbon nanotube-reinforced composite laminated plates", *Acta Mechanica*, **234**, 1687-1711. https://doi.org/10.1007/s00707-022-03438-6.

Dash, S., Mehar, K., Sharma, N., Mahapatra, T.R. and Panda, S.K. (2018), "Modal analysis of FG sandwich doubly curved shell structure. Structural Engineering and Mechanics", *Struct. Eng. Mech.*, **68**(6), 721-733. https://doi.org/10.12989/sem.2018.68.6.721.

Eghbali, M. and Hosseini, S.A. (2023), "On moving harmonic load and dynamic response of carbon nanotube-reinforced composite beams using higher-order shear deformation theories", *Mech. Adv. Compos. Struct.*, **10**(2), 257-270. https://doi.org/10.22075/MACS.2022.28205.1431.

El Meiche, N., Tounsi, A., Ziane, N. and Mechab, I. (2011), "A new hyperbolic shear deformation theory for buckling and vibration of functionally graded sandwich plate", *Int. J. Mech. Sci.*, **53**(4), 237-247. https://doi.org/10.1016/j.ijmecsci.2011.01.004.

Gao, W., Liu, Y., Qin, Z. and Chu, F. (2022), "Wave propagation in smart sandwich plates with functionally graded nanocomposite porous core and piezoelectric layers in multi-physics environment", *Int. J. Appl. Mech.*, **14**(7), 2250071. https://doi.org/10.1142/S1758825122500715.

Garg, A., Chalak, H.D., Zenkour, A.M., Belarbi, M.O. and Sahoo, R. (2022), "Bending and free vibration analysis of symmetric and unsymmetric functionally graded CNT reinforced sandwich beams containing softcore", *Thin Wall. Struct.*, **170**, 108626. https://doi.org/10.1016/j.tws.2021.108626.

Gholami, M., Gorji Azandariani, M., Najat Ahmed, A. and Abdolmaleki, H. (2023), "Proposing a dynamic stiffness method for the free vibration of bi-directional functionally-graded timoshenko nanobeams", *Adv. Nano Res.*, **14**(2), 127-139. https://doi.org/10.12989/.2023.14.2.127.

Hadji, L. and Avcar, M. (2021), "Free vibration analysis of FG porous sandwich plates under various boundary conditions", *J. Appl. Comput. Mech.*, **7**(2), 505-519. https://doi.org/10.22055/JACM.2020.35328.2628.

Hatami, S., Ronagh, H.R. and Azhari, M. (2008), "Exact free vibration analysis of axially moving viscoelastic plates", *Comput. Struct.*, **86**(17-18), 1738-1746. https://doi.org/10.1016/j.compstruc.2008.02.002.

Hosseini, H.S., Khorshidi, K. and Payandeh, H. (2009), "Vibration analysis of moderately thick rectangular plates with internal line support using the Rayleigh-Ritz approach", *Scientia Iranica*, **16**(1), 22-39.

Kumar, V., Singh, S.J., Saran, V.H. and Harsha, S.P. (2021), "Exact solution for free vibration analysis of linearly varying thickness FGM plate using Galerkin-Vlasov's method", *Proceedings of the Institution of Mechanical Engineers, Part L: Journal of Materials: Design and Applications*, **235**(4), 880-897.

https://doi.org/10.1177/1464420720980491.
Li, Q., Iu, V.P. and Kou, K.P. (2008), "Three-dimensional vibration analysis of functionally graded material sandwich plates", *J. Sound Vib.*, **311**(1-2), 498-515. https://doi.org/10.1016/j.jsv.2007.09.018.
Malik, M. and Bert, C.W. (1998), "Three-dimensional elasticity solutions for free vibrations of rectangular plates by the differential quadrature method", *Int. J. Solids Struct.*, **35**(3-4), 299-318. https://doi.org/10.1016/S0020-7683(97)00073-5.
Marandi, S.M. and Karimipour, I. (2023), "Free vibration analysis of a nanoscale FG-CNTRCs sandwich beam with flexible core: Implementing an extended high order approach", *Eng. Struct.*, **276**, 115320. https://doi.org/10.1016/j.engstruct.2022.115320.
Meksi, R., Benyoucef, S., Mahmoudi, A., Tounsi, A., Adda Bedia, E.A. and Mahmoud, S.R. (2019), "An analytical solution for bending, buckling and vibration responses of FGM sandwich plates", *J. Sandw. Struct. Mater.*, **21**(2), 727-757. https://doi.org/10.1177/1099636217698443.
Mousavi, S.B., Amir, S., Jafari, A. and Arshid, E. (2021), "Analytical solution for analyzing initial curvature effect on vibrational behavior of PM beams integrated with FGP layers based on trigonometric theories", *Adv. Nano Res.*, **10**(3), 235-251. https://doi.org/10.12989/anr.2021.10.3.235.
Reddy, J.N. (2003), *Mechanics of Laminated Composite Plates and Shells: Theory and Analysis*, CRC press.
Riahi, F., Mamghaderi, V., Zirakian, T. and Sanaati, B. (2019), "Further assessment of buckling stability of steel plates", *Int. J. Civil Eng. Technol.*, **10**(4), 1715-1721.
Rout, M. and Hota, S.S. (2023), "Geometrically nonlinear free vibration of CNTs reinforced sandwich conoidal shell in thermal environment", *Acta Mechanica*, 1-18. https://doi.org/10.1007/s00707-023-03508-3.
Soltani, M.R., Hatami, S., Azhari, M. and Ronagh, H.R. (2016), "Dynamic stiffness method for free vibration of moderately thick functionally graded plates", *Mech. Adv. Compos. Struct.*, **3**(1), 15-30. https://doi.org/10.22075/macs.2016.404.
Soni, S.K., Thomas, B., Swain, A. and Roy, T. (2022), "Functionally graded carbon nanotubes reinforced composite structures: An extensive review", *Compos. Struct.*, **299**, 116075. https://doi.org/10.1016/j.compstruct.2022.116075.
Talebi, S., Arvin, H. and Beni, Y.T. (2023), "Thermal free vibration examination of sandwich piezoelectric agglomerated randomly oriented CNTRC Timoshenko beams regarding pyroelectricity", *Eng. Anal. Bound. Elem.*, **146**, 500-516. https://doi.org/10.1016/j.enganabound.2022.11.013.
Thai, H.T., Nguyen, T.K., Vo, T.P. and Lee, J. (2014), "Analysis of functionally graded sandwich plates using a new first-order shear deformation theory", *Eur. J. Mech. A Solids*, **45**, 211-225. https://doi.org/10.1016/j.euromechsol.2013.12.008.
Timoshenko, S. and Woinowsky-Krieger, S. (1959), *Theory of Plates and Shells*, McGraw-hill, New York.
Wittrick, W.H. and Williams, F.W. (1974), "Buckling and vibration of anisotropic or isotropic plate assemblies under combined loadings", *Int. J. Mech. Sci.*, **16**(4), 209-239. https://doi.org/10.1016/0020-7403(74)90069-1.
Wolfram Research, Inc. (2024), Mathematica, Version 14.0, Champaign, IL, U.S.A. https://www.wolfram.com
Wu, H., Kitipornchai, S. and Yang, J. (2015), "Free vibration and buckling analysis of sandwich beams with functionally graded carbon nanotube-reinforced composite face sheets", *Int. J. Struct. Stabil. Dyn.*, **15**(7), 1540011. https://doi.org/10.1142/S0219455415400118.
Wu, X. and Fang, T. (2022), "Intelligent computer modeling of large amplitude behavior of FG inhomogeneous nanotubes", *Adv. Nano Res.*, **12**(6), 617-627. https://doi.org/10.12989/anr.2022.12.6.617.
Yang, Z. and He, D. (2019), "Vibration and buckling of functionally graded sandwich micro-plates based on a new size-dependent model", *Int. J. Appl. Mech.*, **11**(1), 1950004. https://doi.org/10.1142/S1758825119500042.
Yang, Z., Wu, P., Liu, W. and Fang, H. (2020), "Analytical solutions for functionally graded sandwich plates bonded by viscoelastic interlayer based on kirchhoff plate theory", *Int. J. Appl. Mech.*, **12**(6), 2050062. https://doi.org/10.1142/S1758825120500623.
Zenkour, A.M. (2005), "A comprehensive analysis of functionally graded sandwich plates: Part 2—Buckling and free vibration", *Int. J. Solids Struct.*, **42**(18-19), 5243-5258. https://doi.org/10.1016/j.ijsolstr.2005.02.016.
Zhao, J.L., Chen, X., She, G.L., Jing, Y., Bai, R.Q., Yi, J., Pu, H.Y. and Luo, J. (2022), "Vibration characteristics of functionally graded carbon nanotube-reinforced composite double-beams in thermal environments", *Steel Compos. Struct*, **43**(6), 797-808. https://doi.org/10.12989/scs.2022.43.6.797.

JL